Stem Cell Research 48 (2020) 101972

Contents lists available at ScienceDirect

Stem Cell Research

journal homepage: www.elsevier.com/locate/scr

# Calreticulin regulates Src kinase in osteogenic differentiation from embryonic stem cells

Zahra Alvandi*[,1], Layla J.R Al-Mansoori[2], Michal Opas

*Department of Lab Medicine & Pathobiology, University of Toronto, Toronto, ON M5S1A8, Canada*

A B S T R A C T

Calreticulin, the major $Ca^{2+}$ buffer of the endoplasmic reticulum plays an important role in the choice of fate by embryonic stem cells. Using the embryoid body method of organogenesis, we showed impaired osteogenesis in $crt^{-/-}$ cells *vis-à-vis* calreticulin-containing osteogenic WT cells. In the non-osteogenic $crt^{-/-}$ cells, c-Src- a non-receptor tyrosine kinase- was activated and its inhibition rescued osteogenesis. Most importantly, we demonstrated that calreticulin-containing cells had lower c-Src kinase activity, and this was accomplished *via* the $Ca^{2+}$-homeostatic function of calreticulin. Specifically, lowering cytosolic $[Ca^{2+}]$ in calreticulin-containing osteogenic WT cells with BAPTA-AM, activated c-Src and impaired osteogenic differentiation. Conversely, increasing cytosolic $[Ca^{2+}]$ in $crt^{-/-}$ cells with ionomycin deactivated c-Src kinase and restored osteogenesis. The immediate effector of calreticulin, the Ser/Thr phosphatase calcineurin, was less active in $crt^{-/-}$ cells, however, its activity was rescued upon inhibition of c-Src activity by small molecule inhibitors. Finally, we showed that higher activity of calcineurin correlated with increased level of nuclear Runx2, a transcription factor that is the master regulator of osteogenesis. Collectively, our work has identified a novel pathway involving calreticulin regulated $Ca^{2+}$ signalling via c-Src in osteogenic differentiation of embryonic stem cells.

## 1. Introduction

Calreticulin (CRT) is an endoplasmic reticulum (ER)-residing protein that regulates the intracellular $Ca^{2+}$ ($[Ca^{2+}]_i$) homeostasis via its high $Ca^{2+}$ storage capacity (Nishida, 1983; Toyoshima et al., 1986; Michalak et al., 2009). Calreticulin plays an important role in embryonic stem (ES) cell differentiation and development (Groenendyk and Michalak, 2014; Karimzadeh and Opas, 2017; Papp et al., 2009; Szabo et al., 2009; Pilquil et al., 2020). While calreticulin deficiency is lethal in utero due to impaired cardiac development, over-expression of constitutively active calcineurin (CaN; a Ca2 + -regulated Ser/Thr phosphatase) in the hearts of calreticulin deficient mice is able to rescue them from embryonic lethality, making it possible to study live, calreticulin deficient animals (Guo, 2002; Lynch and Michalak, 2003). As such, calcineurin has been shown to be one of calreticulin's effectors via calreticulin's intracellular Ca2+ homeostatic functions (Lynch and Michalak, 2003; Lynch, 2005; Lynch et al., 2006). In addition, gain- and loss-of-function experiments indicated that higher calcineurin expression is positively correlated with osteoblastic differentiation and bone formation in mice, although the potential mechanisms have not been fully elucidated (Pilquil et al., 2020; Sun, 2005; Tomita et al., 2002; Winslow, 2006). Together these findings underscore the significance of the calreticulin/Ca2+/calcineurin signalling axis in osteogenic differentiation.

We recently demonstrated that calreticulin regulates ES cell (ESC) osteogenic differentiation, where loss of calreticulin reduces osteogenic differentiation (Pilquil et al., 2020). Src family kinases play crucial roles in regulating cellular adhesion, growth, migration, and differentiation (Parsons and Parsons, 2004). c-Srchas been shown to increase the rate of bone resorption in mice (Soriano et al., 1991) and to decrease osteoblast differentiation *in vitro* (Cornelese-ten Velde et al., 1988; D'Souza et al., 1988). It has been shown that the loss or underexpression of calreticulin increases total tyrosine phosphorylation levels (Khatami et al., 1986). c-Src was shown to be highly activated by loss of calreticulin in fibroblasts (Papp et al., 2007, 2008). However, while the inhibitory role of c-Src in osteogenesis has been studied (D'Souza et al., 1988), the effects of c-Src on osteoblast differentiation downstream of calreticulin is unclear.

In the present study, we demonstrate that in the absence of calreticulin, osteogenic differentiation of calreticulin-deficient ($crt^{-/-}$) mouse ESCs (mESCs) is impaired compared to wild type (WT) mESCs. c-Src activity is increased in $crt^{-/-}$ mESCs and, importantly, c-Src activity is shown to be regulated by $[Ca^{2+}]_I$, such that lowering of $[Ca^{2+}]_i$ results in increased c-Src activity. The absence of calreticulin inhibits the activity of calcineurin and activates c-Src, which results in inhibition of the nuclear translocation of the master osteogenic transcription factor, runt-domain related transcription factor 2 (Runx2). This suggests a novel mechanism in which c-Src regulates mESCs osteogenic differentiation via the effects on Runx2 subcellular trafficking, downstream of calreticulin.

* Corresponding author.
*E-mail address:* Zahra.alvandi@childrens.harvard.edu (Z. Alvandi).
[1] Present Address: Department of Vascular Biology, Boston Children's Hospital, Boston, MA, 02115, USA and the Department of Surgery, Harvard Medical School, Boston, MA 02115, USA.
[2] Present Address: Biomedical Research Center, Qatar University, P.O. Box 14924, Doha, Qatar.

https://doi.org/10.1016/j.scr.2020.101972
Received 27 July 2019; Received in revised form 16 June 2020; Accepted 25 August 2020
Available online 01 September 2020
1873-5061/ © 2020 The Authors. Published by Elsevier B.V. This is an open access article under the CC BY license (http://creativecommons.org/licenses/BY/4.0/).

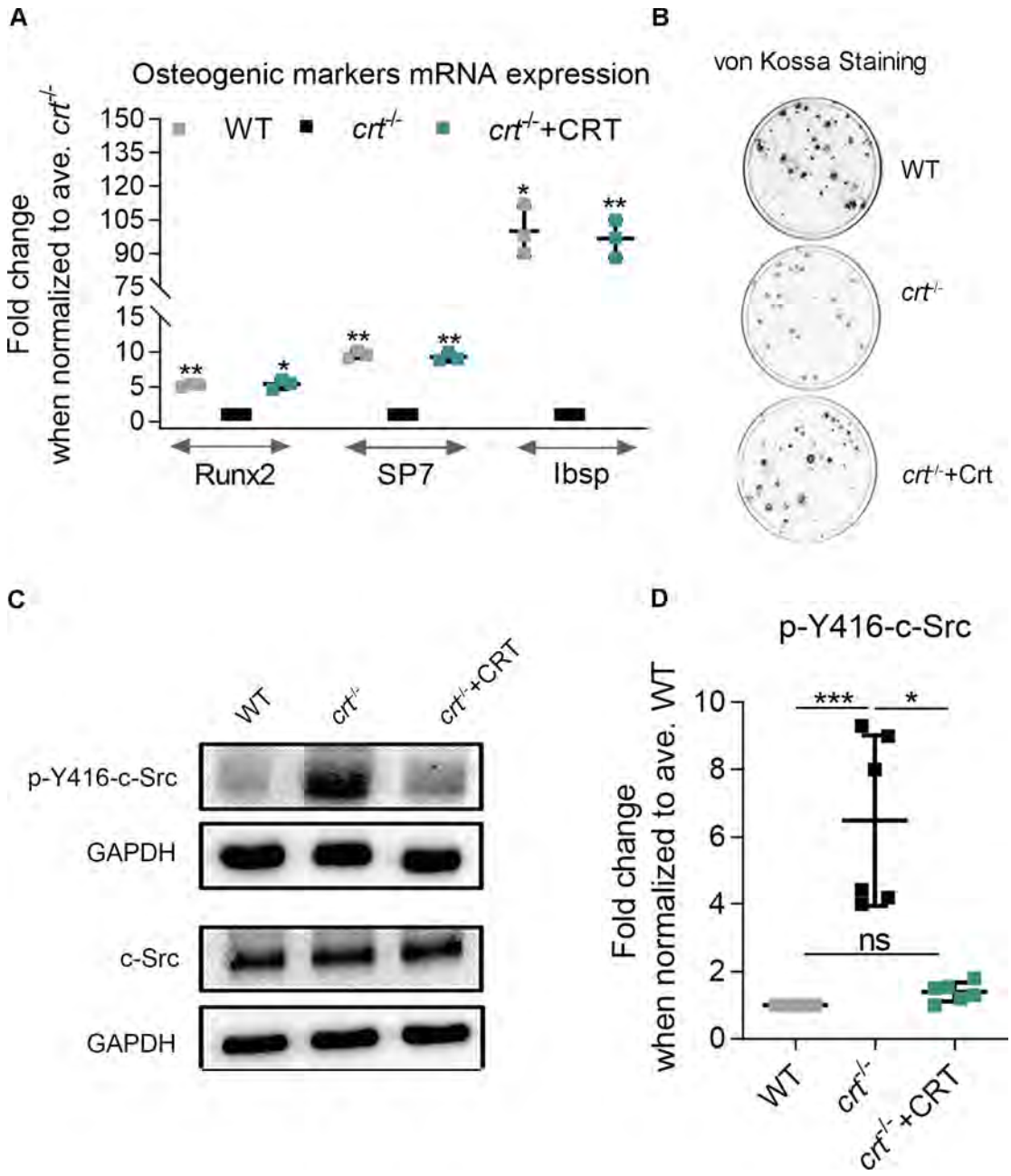


**Fig. 1. c-Src activity is increased in the absence of calreticulin expression in WT mESCs.** (**A**) Effect of calreticulin on expression of osteogenic markers mRNA. Total RNA was extracted from day 21 nodules differentiated from WT, $crt^{-/-}$, and $crt^{-/-}$ + Crt ESCs and subjected to qPCR analysis using Runx2, SP7, and Ibsp primer pairs. mRNA expression was calculated by normalizing ct values to L32 housekeeping gene. Fold change was calculated when values were normalized against corresponding $crt^{-/-}$ values. Data expressed as means ± SD, and n of minimum 3, and two-way ANOVA analysis among WT, $crt^{-/-}$, and $crt^{-/-}$ + CRT ESCs results: $F = 154.9$, $p < 0.0001$. Bonferroni post hoc analysis as indicated: *$p < 0.05$, **$p < 0.01$. (**B**) Mineralization of mESCs in the absence and presence of calreticulin expression assessed by von Kossa staining. Mineralized deposits of Day 21 nodules differentiated from WT, $crt^{-/-}$, and $crt^{-/-}$ + Crt ESCs using osteogenic protocol were stained by von Kossa method. (**C**) c-Src activity in mESCs in the presence and absence of calreticulin. p-Y416-c-Src levels and levels of total c-Src were examined in immunoblots. GAPDH served as loading control. (**D**) Quantification of western blot analysis. p-Y416-c-Src band densities were quantified using ImageJ. Normalized values to corresponding total c-Src representing the mean ( ± SD) were graphed and subjected to Kruskal-Wallis test ($p < 0.0001$). Multiple comparisons were performed where each comparison stands individually using Dunnett's test and indicated as *$p < 0.05$ and *** < 0.005.

## 2. Materials and methods

### 2.1. Cell culture

Mouse embryonic stem cell lines used in the study (WT, $crt^{-/-}$ and $crt^{-/-}$ + Crt, and $crt^{-/-}$ + CaN) were maintained in LIF containing medium. Osteogenic differentiation was performed via the hanging drop method using an optimized protocol developed in our laboratory (Yu et al., 2016). 250 cells per 25 μL drops were placed on the lids of tissue culture dishes for 3 days. The medium consisted of high glucose Dulbecco modified Eagle's medium with sodium pyruvate and L-glutamine, 20% FBS, nonessential amino acids, and β-mercaptoethanol. After 3 days in hanging drop, ES cell aggregates called EBs were then floated in differentiation medium containing 0.1 μM retinoic acid for 2 days. On day 5, the EBs were plated in tissue culture dishes coated with 0.1% gelatin in PBS. Retinoic acid was added in the media for the entire duration of the EBs in floating stage. On day 6, the differentiation medium was supplemented with 50 μg/mL ascorbic acid and 10 mM β-

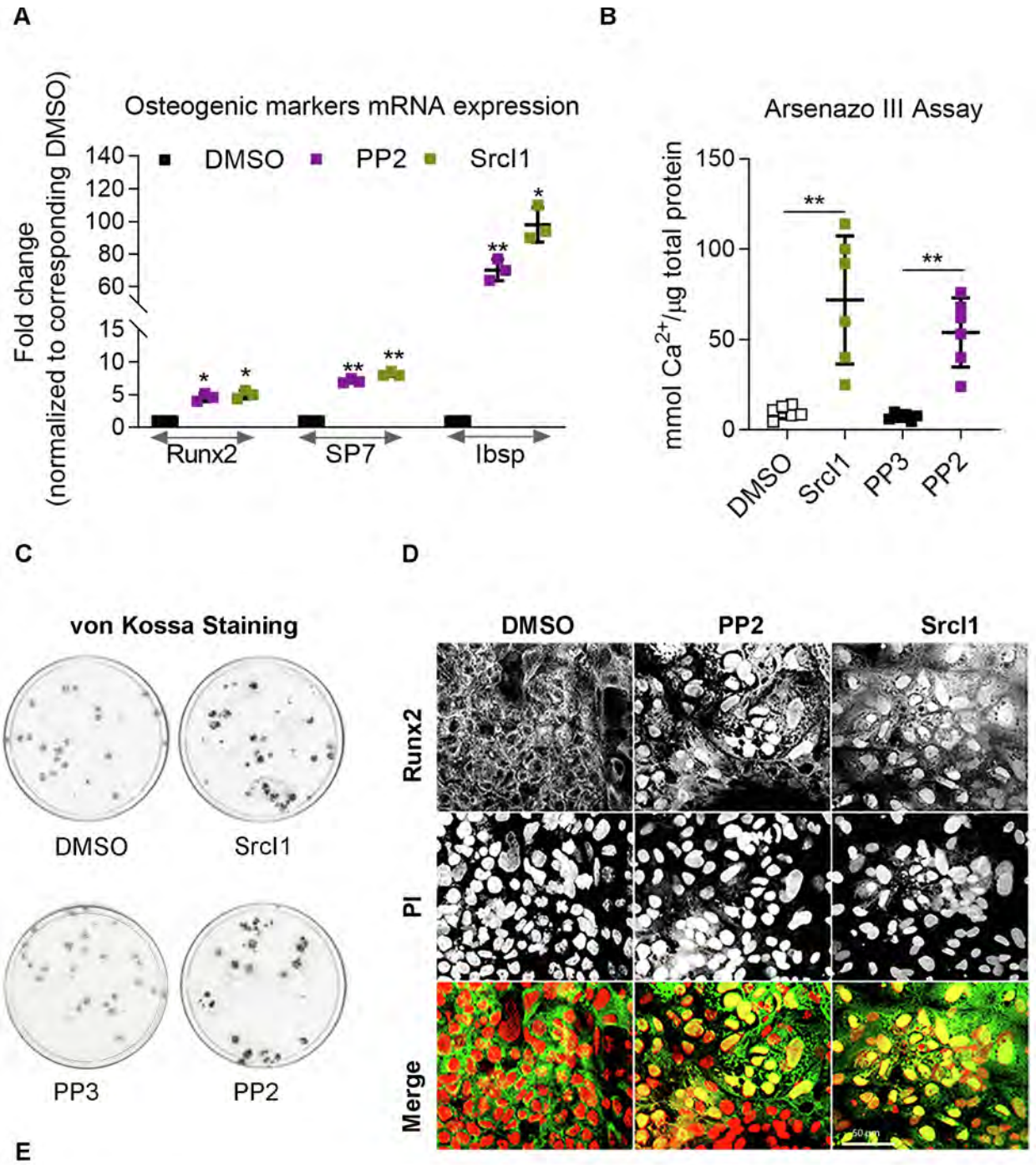


E

| | DMSO | PP2 | Srcl1 |
|---|---|---|---|
| Pearson's correlation coefficient (Mean ± SD) | -0.461 ± 0.33 | 0.472 ± 0.089 | 0.645 ± 0.093 |
| Mander's overlap coefficients (Mean ± SD) | 0.257 ± 0.087 | 0.808 ± 0.025 | 0.883 ± 0.029 |

*(caption on next page)*

glycerophosphate for commitment to the osteogenic lineage. Dexamethasone (100 nM) was added on day 10 to further enrich cells of the osteogenic lineage. The medium was changed every 2 days for the entire 21 days of differentiation.

### 2.2. Inhibition assays

Ionomycin (Sigma-Aldrich, Catalog No. I3909) and BAPTA-AM (Sigma-Aldrich, Catalog No. A1076) treatments were performed. To chelate cytosolic Ca2+, floating EBs were incubated with 0.1 µM

**Fig. 2. Inhibition of c-Src activity in $crt^{-/-}$ cells improved osteogenic differentiation.** (**A**) c-Src inhibition and its effect on osteogenic markers mRNA expression. Total RNA was extracted from day 21 nodules differentiated from WT, $crt^{-/-}$, and $crt^{-/-}$ + Crt ESCs under osteogenic protocol and analysed by qPCR using Runx2, SP7, and Ibsp primer pairs. mRNA expression was calculated by normalizing values to L32 housekeeping gene. Fold change was calculated when values were normalized to their corresponding DMSO condition. Values representing the mean ( ± SD) of triplicates were graphed and subjected to two-way ANOVA; F = 196.3, $p < 0.0001$. Bonferroni post hoc analysis as indicated: *$p < 0.05$, **$p < 0.01$. (**B**) c-Src inhibition and its effect on mineralization of non-osteogenic $crt^{-/-}$ mESCs assessed by Arsenazo III staining. Day 21 nodules of $crt^{-/-}$ with the indicated treatments were stained by Arsenazo III method. The absorbance of the Ca-Arsenazo III complex was measured dichromatically at 660/700 nm. Values representing the mean ( ± SD) of six measurements were graphed and subjected to Kruskal-Wallis test ($p = 0.0004$). Planned comparison were made between DMSO and SrcI1 treated cells and PP3 vs. PP2 treated cells using Dunnett's test. **$p < 0.01$. (**C**) c-Src inhibition and its effect on mineralization outcome of osteogenic differentiation in $crt^{-/-}$ mESCs assessed by von Kossa. Day 21 nodules of the indicating cells were stained by von Kossa method to assess the mineralized deposits under each treatment condition. representing the mean ( ± SD) of triplicates were graphed and subjected to one-way ANOVA. (**D**) Runx2 subcellular localization upon inhibition of c-Src activity. differentiating EBs from $crt^{-/-}$ mESCs treated with c-Src inhibitors (PP2 and SrcI1) and the solvent control DMSo were subjected to immunofluorescence staining using anti Runx2 antibody (Green). Confocal immunofluorescence localization analysis of Runx2 trafficking in differentiating EBs from $crt^{-/-}$ mESCs treated with c-Src inhibitors (PP2 and SrcI1) and the solvent control DMSO. Dual channel grey level images of a single field are displayed with the top rows showing RUNX2 immunolocalization, PI-labelled nuclei in the middle row and the merged RGB images in the bottom rows. Scale bar = 50 μm. (**E**) Pearson's and Manders' coefficients should be interpreted as follows: Pearson's correlation coefficient returns values from + 1 to −1 with + 1 for perfect correlation (colocalization), 0 for no correlation, and −1 for total anti-correlation. Manders' overlap coefficient measures positions and intensities of fluorescence of pixels in each colour channel. It returns values ranging from 1 to 0, thus showing full colocalization or no colocalization, respectively. (For interpretation of the references to colour in this figure legend, the reader is referred to the web version of this article.)

BAPTA-AM for 30 min each day at days 3–5 of differentiation. To increase cytosolic Ca2+, the EBs were incubated with 1 μM ionomycin for 2 h each day in the same manner. For inhibition of calcineurin, floating EBs were incubated with 1 μg/ml cyclosporin-A (for 2 h). c-Src inhibitor PP2 (Calbiochem, Catalog No. 529573), SrcI1 (Sigma, Catalog No. S2075), and negative control PP3 (Calbiochem, Catalog No. 529574) were applied based on survey by Bain *et al.* (Bain et al., 2003) at 10uM and 1uM each day between day 3 to 5, respectively.

### 2.3. Calcineurin activity assay

Calcineurin activity assay was carried out as previously described (Fruman et al., 1992). Briefly, a peptide corresponding to the regulatory domain of protein kinase A was used as the substrate in an *in vitro* dephosphorylation assay. Cells ($1.0 \times 10^6$) were lysed in 50 ul of hypotonic lysis buffer and 20 ul of lysate was added to $^{32}$P-labeled RII-peptide (300 pmols). The reaction was carried out for 15 min at 30°C and number of pmols released phosphate was calculated. Activity of calcineurin was expressed in pmols of phosphate released per minute per mg of total protein.

### 2.4. Mineral deposition assays

Differentiated day 21 nodules were examined for the presence of mineral deposits using von Kossa and Arsenazo III staining as performed in previous studies (Bellows et al., 1986). Briefly, for von Kossa staining, cells were rinsed three times with PBS, fixed in 10% neutral formalin buffer for 2 hr, then washed 3 times with distilled water. Nodules were then stained with 2.5% silver nitrate solution for 30 min. After, they were washed 3 times with distilled water and were examined for presence of mineralization. For Arsenazo III staining, the amount of $Ca^{2+}$ in the matrix was measured using Arsenazo III (Sigma) staining method as previously described (Michaylova and Ilkova, 1971).

### 2.5. Real-time PCR analysis

The Qiagen RNeasy Mini Kit was used to extract total RNA from day 21 nodules according to the manufacturer's instructions. 4 μg of RNA was reverse transcribed to cDNA using Superscript II (Invitrogen) in a total reaction volume of 48 μL. Real-time PCR analysis was performed in Bio-Rad's CFX384 Touch detection system. The primer sequences that were designed and used are as follows: for L32, forward primer 5′-CATGGCTGCCCTTCGGCCTC-3′ and reverse primer 5′-CAT TCTCTTCGCTGCGTAGCC-3′;for RUNX2, forward primer 5′- CCTCTG ACTTCTGCCTCTGG-3′ and reverse primer 5′-TAAAGGTGGCTGGGTA GTGC-3′;

for SP7, forward primer 5′-AAGTCCCACACAGCAGCTG-3′ and reverse primer 5′- AGCCGAGCTGCCAGAGTTTG-3′; and for Ibsp, forward primer 5′- AACAATCCGTGCCACTCA-3′ and reverse primer 5′-GGAGG GGGCTTCACTGAT-3′.

### 2.6. SDS-PAGE and western blot analysis

Cells were collected in a lysis buffer containing 50 mM Tris-HCl, pH 8.0, 120 mM NaCl, and 0.5% NP-40. 30 ug lysates per lane were separated by SDS-PAGE and transferred to nitrocellulose membrane. The following primary antibodies were used: anti-c-Src (Cell Signaling, Catalog No. 2108), anti-p-c-Src-Y416 (Cell Signaling, Catalog No.2101S), anti- Runx2 (Cell Signaling, Catalog No.8486S), and anti-GAPDH (Cell Signaling, Catalog No.2118S) antibodies. The secondary antibody used was Goat polyclonal Secondary Antibody to Rabbit IgG - H&L (HRP) (Abcam, Catalog No. ab6721). Immunoreactive bands were detected using the DNR MicroChem chemiluminescence camera system (DNR Bio-Imaging Systems) and were quantified using ImageJ (developed by Wayne Rasband, NIH, https://imagej.nih.gov/ij/) where indicated.

### 2.7. Immunofluorescence staining

Day 21 nodules on coverslips were rinsed 3 times with PBS, and fixed in 3.7% formaldehyde for 15 min. After washing in PBS, the cells were permeabilized with 0.1% Triton X-100 in buffered containing 100 mM 1,4- piperazinediethanesulfonic acid, 1 mM EGTA, and 4% (wt/vol) polyethylene glycol 8000 (pH 6.9) for 2 min. Nodules were then washed by PBS and were incubated with 1:50 dilution of anti-Runx2 (Abcam, Catalog No. ab76956) at 4°C overnight. After washing in PBS (3 times for 5 min), the cells were stained with the secondary antibody diluted 1:1000 for 1hr at room temperature. For nuclear staining, 500 nM PI solution was added to cover the nodules for 5 min. After final rinsing in PBS, the slides were mounted in fluorescent mounting medium (Dako, Catalog No. S3023). A confocal fluorescence microscope (MRC 600; Bio-Rad Laboratories) equipped with a 60/1.40 plan Apochromatic oil immersion objective (Nikon) and krypton-argon laser was used for fluorescence imaging. COSMOS software (Bio-Rad Laboratories) was used for image acquisition.

### 2.8. Image and Statistical analysis

Mander's and Pearson's coefficients were calculated using ImageJ freeware [https://imagej.nih.gov/ij/] from a minimum of three random fields of view. Manders' overlap coefficient measures positions and intensities of fluorescence of pixels in each colour channel. It returns values ranging from 1 to 0, thus showing full colocalization or no co-localization, respectively. Pearson's correlation coefficient is not

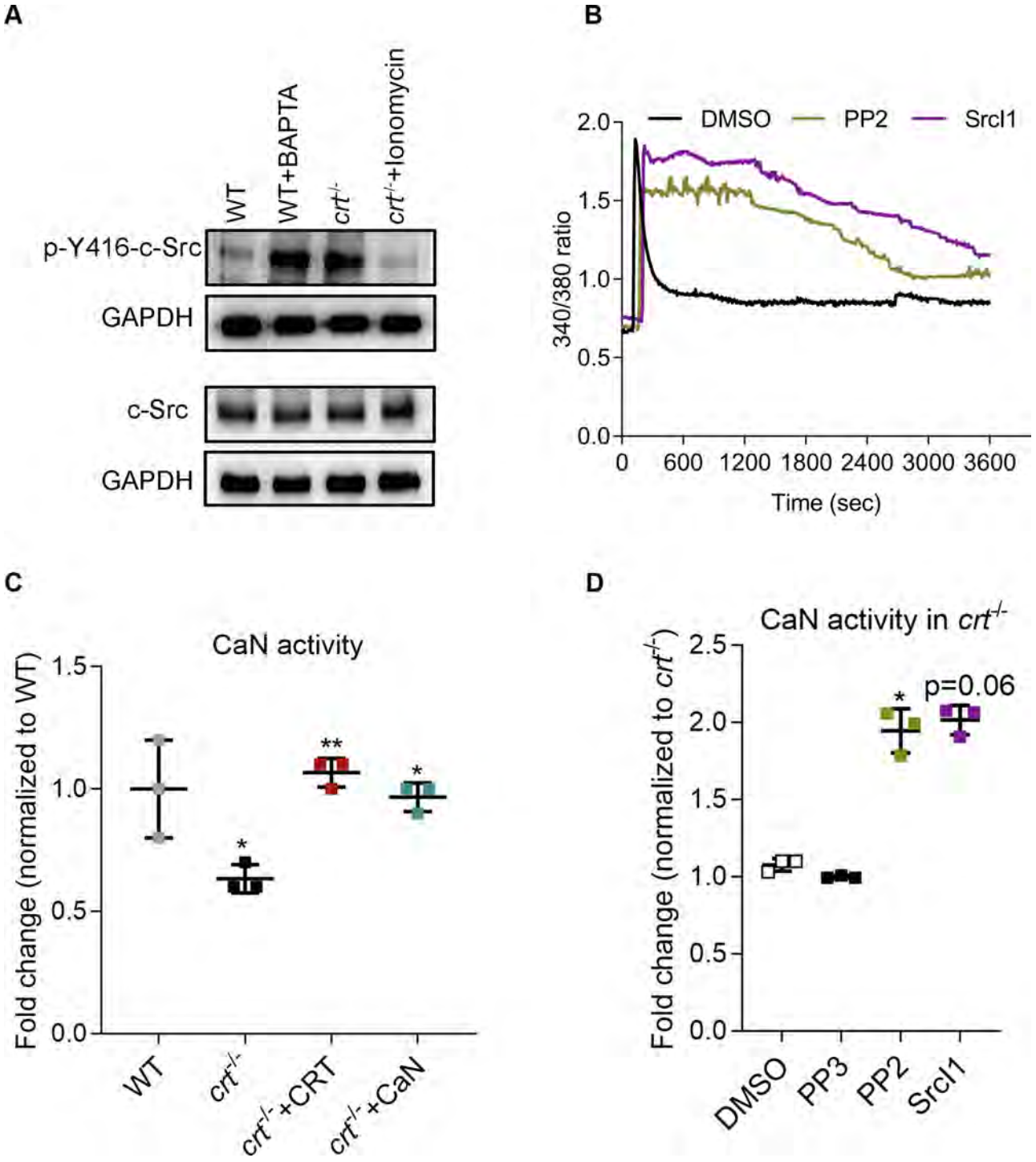


**Fig. 3. Calreticulin (CRT) regulates Src kinase activity through its calcium homeostasis function.** (**A**) c-Src activity in response to $[Ca^{2+}]_i$ changes. WT (lane 1), WT treated with BAPTA-AM (lane 2), $crt^{-/-}$ (lane 3), and $crt^{-/-}$ treated with ionomycin (lane 4) were western blotted using antibodies for p-Y416-c-Src and c-Src. GAPDH served as loading controls. (**B**) Representative traces of $[Ca^{2+}]_i$ responses to c-Src inhibition in $crt^{-/-}$ mESCs. DMSO was the solvent control. Data represent the mean ( ± SD) of readings from two independent experiments. (**C**) Calcineurin activity comparison among cells in the absence and presence of calreticulin. WT, $crt^{-/-}$, $crt^{-/-}$ + CRT, and $crt^{-/-}$ + CaN mESCs were tested for level of calcineurin activity. Data represent mean ± SD, with significance determined by one-way ANOVA with a Bonferroni's multiple comparison test. *p < 0.05, and **p < 0.01. (**D**) c-Src inhibition and its effect on calcineurin activity in $crt^{-/-}$ mESCs. $crt^{-/-}$ mESCs were treated with c-Src inhibitors including PP2 and SrcI1 prior to calcineurin activity measurements. Control conditions included DMSO (solvent Ctrl) and PP3 (inactive analog of PP2). Values representing the mean ( ± SD) of triplicates were graphed and subjected to Kruskal-Wallis test (p < 0.0001). Planned comparisons were made to compare PP2 and PP3 treated cells, and SrcI1 and DMSO treated cells using Dunn's test. **p < 0.01.

sensitive to differences in mean signal intensities and returns values from + 1 to −1 with + 1 for perfect correlation (colocalization), 0 for no correlation, and −1 for total anti-correlation.

Error bars shown in the figures represent standard deviations and n represents the number of independent experiments performed. Statistical differences between two groups were analyzed by one-way or two-way analysis of variance or non-parametric Kruskal-Wallis test when appropriate using the GraphPad Prism 8.3.0 application.

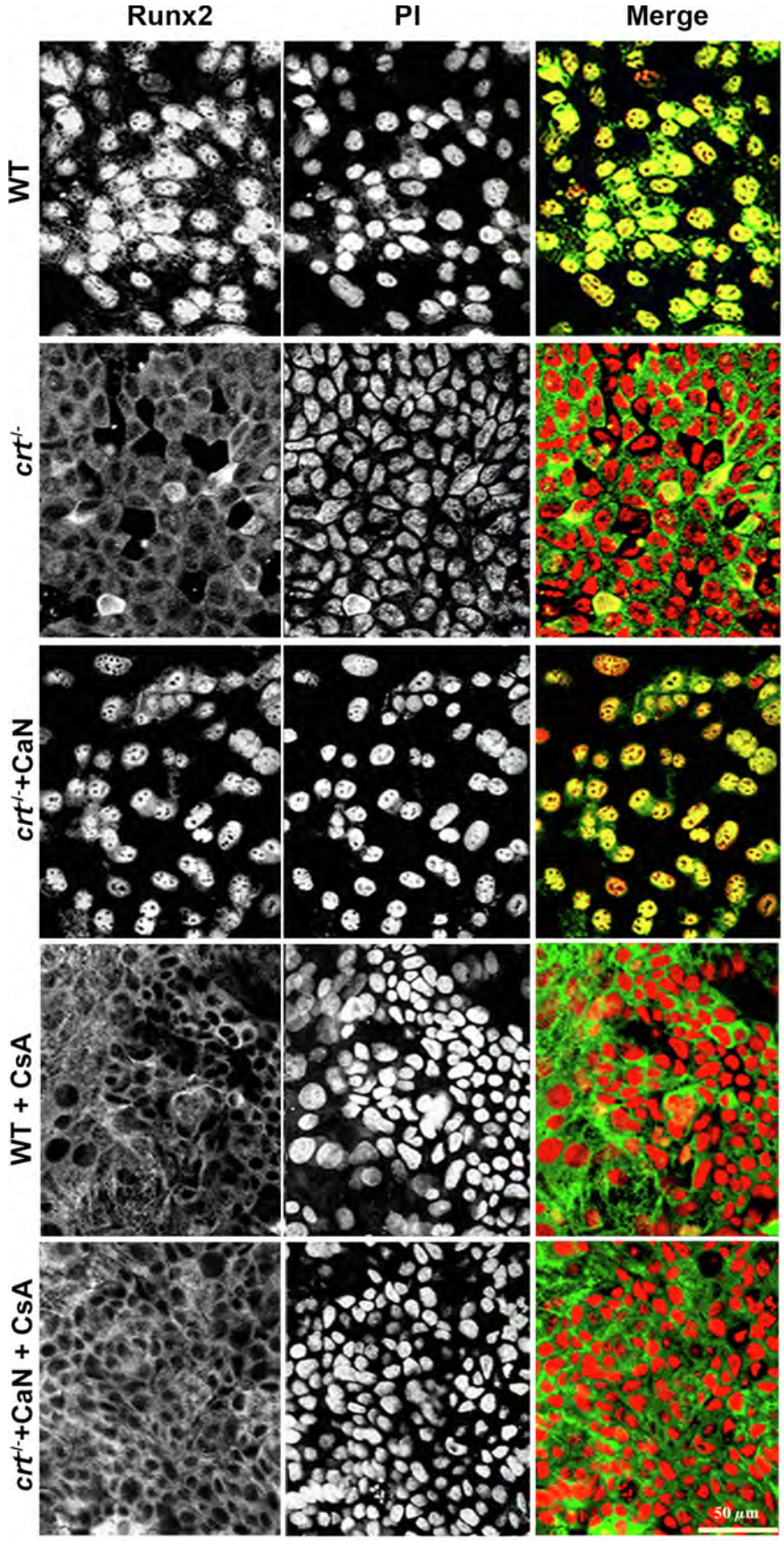


| | WT | crt -/- | crt -/-+CaN | WT+CsA | crt -/-+CaN+ CsA |
|---|---|---|---|---|---|
| Pearson's correlation coefficient (Mean ± SD) | 0.763 ± 0.099 | -0.497 ± 0.137 | 0.889 ± 0.042 | -0.661 ± 0.125 | -0.658 ± 0.148 |
| Mander's overlap coefficients (Mean ± SD) | 0.902 ± 0.32 | 0.245± 0.056 | 0.958 ± 0.016 | 0.346 ± 0.12 | 0.281 ± 0.09 |

**Fig. 4. Calcineurin (CaN) regulates Runx2 nuclear localization downstream of Src.** Runx2 subcellular localization upon inhibition of calcineurin activity. WT, $crt^{-/-}$, $crt^{-/-}$ + CaN, WT treated with cyclosporin A (CsA), and CsA treated $crt^{-/-}$ + CaN mESCs undergoing osteogenic differentiation were immunolabelled using anti Runx2 antibody. Dual channel grey level images of a single field are displayed where Runx2 staining is presented on the farthest left, PI-labelled nuclei in the middle column and the merged RGB images on the farthest right. Scale bar = 50 µm. For description of Pearson's and Manders' coefficients please see legend to Fig. 2E.

## 3. Results and discussion

### 3.1. Higher c-Src activity and lower calreticulin expression were inversely related to osteogenic differentiation of mECs

We have established that c-Src activity is inversely related to the abundance of calreticulin in mesenchymal cells (Papp et al., 2007). Here, we first investigated a relationship between calreticulin expression and osteogenic differentiation. To do so, calreticulin WT, $crt^{-/-}$, and $crt^{-/-}$ transfected with calreticulin expressing vectors ($crt^{-/-}$ + CRT) mESCs were subjected to osteogenic differentiation. Cells were created and maintained as described previously (Papp et al., 2009; Guo, 2002; Lynch, 2005; Mesaeli, 1999; Szabo et al., 2009). Expression of osteogenic markers and mineralization were examined from day 21 cultures by qPCR and von Kossa staining, respectively. The increase in osteoblast activity of calreticulin WT cells during differentiation was reflected in significantly higher transcript levels of osteoblast-specific genes Runx2, Sp7 (osterix), and Ibsp when compared to $crt^{-/-}$ ESCs. These reduced levels of osteogenic markers were rescued in $crt^{-/-}$ + CRT cells (Fig. 1A). In addition to our results in this study, we have recently shown the supporting role of calreticulin in osteogenic differentiation of mouse ESCs, as evidenced by enhanced nuclear osterix expression in calreticulin WT versus $crt^{-/-}$ cells (Pilquil et al., 2020). The mineralization activity of mature osteoblasts which leads to the deposition of calcium phosphate was assessed by von Kossa staining (Owen, 1990; Brauer et al., 2016), in which Silver ions react with calcium phosphate resulting in black precipitates. Based on the staining intensity, we concluded that the level of mineralized deposits in $crt^{-/-}$ D21 nodules were compromised when compared to WT and $crt^{-/-}$ + CRT cells (Fig. 1B).

Next, we examined c-Src kinase activity in the ESCs differentially expressing calreticulin based on the expression level of phosphorylated Src at Y416. Differentiating calreticulin WT, $crt^{-/-}$, and $crt^{-/-}$ + CRT cells under osteogenic conditions were subjected to western blot analysis (Fig. 1C). Level of p-Y416-c-Src were quantified in all tested cells and normalized to the corresponding total c-Src, which showed that $crt^{-/-}$ cells had significantly higher levels of c-Src activity compared to WT cells. Furthermore, the levels of p-Y416-c-Src in $crt^{-/-}$ + CRT cells were close to those of control WT cells (Fig. 1D). The abundance of total c-Src remained unchanged. These results suggested that calreticulin plays a role in the regulation of c-Src activity in mESCs, as opposed to influencing total transcription levels. Furthermore, given the well-established inhibitory role of c-Src in osteogenesis (Marzia, 2000), it is likely that osteogenic differentiation in $crt^{-/-}$ cells is impaired due to higher c-Src activity in these cells.

### 3.2. Inhibition of c-Src activity in $crt^{-/-}$ ESCs improves osteogenic differentiation

To investigate whether or not calreticulin mediates its effect on osteogenic differentiation through regulation of c-Src kinase activity, c-Src activity in $crt^{-/-}$ cells was inhibited using PP2 (10 μM) or Src-I1 (1 μM) inhibitors. DMSO served as solvent control. RNA from D21 nodules was extracted and subjected to qPCR analysis. The level of osteogenic markers, Runx2, SP7, and Ibsp, were rescued following Src inhibition in $crt^{-/-}$ cells (Fig. 2A) and so was their mineralization, as tested by Arsenazo III assay (Fig. 2B) and von Kossa (Fig. 2C). Arsenazo III assay, which revealed that $Ca^{+2}$ deposits in $crt^{-/-}$ nodules treated with c-Src inhibitors were significantly higher compared to control dishes treated with PP3, the inactive analogue of PP2 and DMSO. This is in agreement with earlier observations that c-Src inhibition enhances osteogenic differentiation (Soriano et al., 1991; Marzia, 2000; Id Boufker, 2010; Lee, 2010; Murrills, 2012). Collectively, these results further confirmed that calreticulin affects osteogenic differentiation through the regulation of c-Src activity.

Since elevated c-Src activity in $crt^{-/-}$ cells was shown to be linked to reduced osteogenic differentiation, we wished to investigate the subcellular distribution of Runx2 in $crt^{-/-}$ cells with or without c-Src inhibition. Immunofluorescence staining revealed Runx2 was predominantly located in the cytoplasm of non-osteogenic $crt^{-/-}$ cells, however, upon inhibition of c-Src with either PP2 (10 μM) or SrcI1 (1 μM), the nuclear presence of Runx2 in $crt^{-/-}$ cells became starkly visible (Fig. 2D). From these results, we infer that inhibition of c-Src kinase in $crt^{-/-}$ ESCs imparts on them a capability to undergo efficacious osteogenic differentiation. Both Manders' overlap coefficients and Pearson's correlation coefficient methods were applied to quantify co-localization of Runx2 with propidium iodide (PI) nuclear staining and the summary of the outcome is provided in a table (Fig. 2E). Regulation of various kinase activities by calreticulin have been reported previously (Papp et al., 2008; Czarnowski et al., 2014; Szabo et al., 2007). We have shown that calreticulin affects c-Src activity in mouse fibroblasts and this is $Ca^{2+}$-dependent (Papp et al., 2007). In another study, increased calreticulin expression was linked to lower expression of pERKs in rat cardiomyocytes and it was argued that calreticulin regulates ERK activity (Lee, 2003). Later, it was found that c-Src increases ERK activity in the rat hippocampus (Hu, 2009). However, in the absence of proper gain- and loss-of-function experiments, the direct effect of calreticulin on ERK activity remains unexplored.

### 3.3. Calreticulin regulates Src kinase activity through its calcium homeostasis function

Previously, we showed that in $crt^{-/-}$ mouse embryonic fibroblasts (MEFs), reduced ER $Ca^{2+}$ concentration increased c-Src kinase activity (Papp et al., 2008). More recently, we showed that calreticulin regulates osteoblast specification in a $Ca^{2+}$-dependent manner (Pilquil et al., 2020). In the current study, we asked whether or not calreticulin-dependent Src activity is regulated by the $Ca^{2+}$ buffering function of calreticulin. Therefore, c-Src activity was tested in response to modification of $[Ca^{2+}]_i$ using ionomycin (1 μM) and BAPTA-AM (100 nM). Western blot analysis showed that decreasing cytosolic $[Ca^{2+}]$ with the $Ca^{+2}$ chelator BAPTA-AM enhanced c-Src kinase activity in WT cells (lane 2, Fig. 3A), while increasing cytosolic $[Ca^{2+}]$ with ionomycin in $crt^{-/-}$ cells reduced phosphorylation of c-Src on Y416 (lane 4, Fig. 3A). The abundance of total c-Src remained unchanged. To further assess the effect of c-Src activity on intercellular calcium, $Ca^{2+}$ release in $crt^{-/-}$ cells in response to c-Src inhibition was measured using cell-permeable $Ca^{2+}$-binding fluorescent ratiometric dye Fura-2AM to measure cytosolic free $[Ca^{2+2+}]$. $crt^{-/-}$ cells showed an apparent increase in cytosolic free $[Ca^{2+}]$ when treated with the c-Src inhibitors PP2 and SrcI1 compared to DMSO tread cells (Fig. 3B). Increase in $[Ca^{2+}]_i$ has been shown to activate many calmodulin-dependent enzymes, including calcineurin (Crabtree, 2001; Crabtree and SchreiberSnapShot, 2009). Therefore, it was critical to know how calcineurin activity was affected downstream of calreticulin in ES cells. Our results show that calcineurin activity was significantly reduced in $crt^{-/-}$ cells, however, calcineurin activity in $crt^{-/-}$ + CRT was restored to the WT levels. Moreover, a stable transfection of non-osteogenic $crt^{-/-}$ cells with constitutively active calcineurin ($crt^{-/-}$ + CaN) also restored calcineurin activity to the WT levels (Fig. 3C). Next, we asked whether or not the increase in cytosolic $Ca^{2+}$ level following c-Src inhibition would increase calcineurin activity in the $crt^{-/-}$ cells. Interestingly, c-Src inhibition using either PP2 (10 μM) or SrcI1 (1 μM) inhibitors induced calcineurin activity in $crt^{-/-}$ cells (Fig. 3D). These findings suggest that the inhibitory effect of c-Src in $crt^{-/-}$ cells may be directed through calcineurin.

### 3.4. Calcineurin regulates Runx2 nuclear localization downstream of Src

Our results indicate that calcineurin activity downstream of Src is reduced in $crt^{-/-}$ cells. We show that inhibition of Src kinase activity in $crt^{-/-}$ ES cells enhances the intranuclear translocation of Runx2. Osteo-chondroprogenitor cell commitment to osteoblastic cell lineage

during mesenchymal condensation is regulated by Runx2 (McDonnell et al., 1960; Porrello and LaVail, 1986). Here, we examined Runx2 localization downstream of calcineurin in ES osteogenic differentiation. Runx2 was immunolocalized (Fig. 4) in cells modified with respect to calcineurin activity (Fig. 3C, D). Runx2 was predominantly cytoplasmic in $crt^{-/-}$ ES cells (Fig. 4; $crt^{-/-}$) with lowest activity of calcineurin. Interestingly, with increasing calcineurin activity in WT cells and cells containing constitutively active calcineurin, Runx2 presence became increasingly intranuclear (Fig. 4; WT, and $crt^{-/-}$ + CaN). To confirm that the intranuclear translocation of Runx2 is indeed due to the calcineurin activity, WT and $crt^{-/-}$ + CaN cells were treated with 1 μg/ml of the calcineurin inhibitor cyclosporin A (CsA). Immunolocalization microscopy revealed that upon inhibition of calcineurin activity, trafficking of Runx2 to the nucleus was distinctly attenuated (Fig. 4; WT + CsA, and $crt^{-/-}$ + CaN + CsA).

The significance of calcineurin in osteoblastic bone formation has been studied previously where it showed that calcineurin Aα isoform enhances bone formation (Sun, 2005). In another study, calcineurin/NFAT signaling was found to regulate osteoblast proliferation, osteoclast differentiation, and the coordination of bone formation and resorption (Winslow, 2006). Furthermore, inhibition of Src family kinases was found to enhance NFATc1 nuclear localization and activation (Baer et al., 2017). The authors suggested that the mechanism for increased NFATc1 nuclear translocation in the absence of active Src kinases could depend on calcineurin. Although the aforementioned work tentatively links calcineurin and Src activity, the potential role of calreticulin as an upstream regulator in osteogenesis from ESCs remains poorly characterized. Our data indicate that calcineurin activity downstream of c-Src is likely to regulate intracellular trafficking of Runx2 and hence might control osteogenic differentiation from ES cells. Interestingly, phosphorylation of a conserved serine (S451) on Runx2 was found to negatively regulate Runx2 transcriptional activity (Wee et al., 2002). One could speculate that enhanced phosphatase activity of calcineurin in the presence of calreticulin and inhibition of c-Src activity might result in dephosphorylation of Runx2 at S451. Enhanced transcriptional activity of S541-dephosphorylated Runx2 could in turn enhance osteogenic output during ESC differentiation.

In summary, we have shown here that the osteogenic ability of cells is dependent on the Ca2 + homeostatic function of calreticulin, which influences (reduces) c-Src activity. Downstream calcineurin activity is thereby also affected, such that in cells harbouring calreticulin, calcineurin activity is intact and Runx2, the master osteogenic transcription factor, is properly localized to the nucleus. The opposite scenario is true for calreticulin deficient cells, which have a decreased osteogenic ability, but which was shown to be rescued here by a variety of means, including c-Src inhibition and cytosolic Ca2+ increase. Thus, our results show that calreticulin is a crucial regulator in the osteogenic signalling pathway.

## CRediT authorship contribution statement

**Zahra Alvandi:** Formal analysis, Data curation, Writing - original draft, Writing - review & editing, Visualization. **Layla J.R Al-Mansoori:** Conceptualization, Methodology, Formal analysis, Data curation, Investigation, Validation, Visualization. **Michal Opas:** Conceptualization, Methodology, Formal analysis, Data curation, Writing - original draft, Writing - review & editing, Investigation, Visualization, Supervision, Funding acquisition, Project administration.

## Declaration of Competing Interest

The authors declare that they have no known competing financial interests or personal relationships that could have appeared to influence the work reported in this paper.

## Acknowledgements

We are grateful to Dr. Sylvia Papp and Dr. Peter Dziak for critical comments on the manuscript. We also thank Amirhossein Alvandi for his consultations regarding the statistical analysis of this study. M.O. is a member of the Ontario Stem Cell Initiative and a member of the Heart & Stroke/Richard Lewar Centre of Excellence. This work was supported by grants from CIHR MOP-130551 and MOP-106461 to M.O.

## References

Baer, A., Colon-Moran, W., Xiang, J., Stapleton, J.T., Bhattarai, N., 2017. Src-family kinases negatively regulate NFAT signaling in resting human T cells. PloS One 12, e0187123. https://doi.org/10.1371/journal.pone.0187123.

Bain, J., McLauchlan, H., Elliott, M., Cohen, P., 2003. The specificities of protein kinase inhibitors: an update. Biochem. J. 371, 199–204. https://doi.org/10.1042/bj20021535.

Bellows, C.G., Aubin, J.E., Heersche, J.N., Antosz, M.E., 1986. Mineralized bone nodules formed in vitro from enzymatically released rat calvaria cell populations. Calcif. Tissue Int. 38, 143–154. https://doi.org/10.1007/bf02556874.

Brauer, A., Pohlemann, T., Metzger, W., 2016. Osteogenic differentiation of immature osteoblasts: Interplay of cell culture media and supplements. Biotechnic Histochem. Off. Publicat. Biol. Stain Commiss. 91, 161–169. https://doi.org/10.3109/10520295.2015.1110254.

Cornelese-ten Velde, I., Bonnet, J., Tanke, H.J., Ploem, J.S., 1988. Reflection contrast microscopy. Visualization of (peroxidase-generated) diaminobenzidine polymer products and its underlying optical phenomena. Histochemistry 89, 141–150. https://doi.org/10.1007/bf00489917.

Crabtree, G.R., 2001. Calcium, calcineurin, and the control of transcription. J. Biol. Chem. 276, 2313–2316. https://doi.org/10.1074/jbc.R000024200.

Crabtree, G.R., SchreiberSnapShot, S.L., 2009. Ca2+-calcineurin-NFAT signaling. Cell 138 (210). https://doi.org/10.1016/j.cell.2009.06.026. 210.e211.

Czarnowski, A., Papp, S., Szaraz, P., Opas, M., 2014. Calreticulin affects cell adhesiveness through differential phosphorylation of insulin receptor substrate-1. Cellul. Mol. Biol. Lett. 19, 77–97. https://doi.org/10.2478/s11658-014-0181-9.

D'Souza, S.E., Ginsberg, M.H., Burke, T.A., Lam, S.C., Plow, E.F., 1988. Localization of an Arg-Gly-Asp recognition site within an integrin adhesion receptor. Science (New York N.Y.) 242, 91–93. https://doi.org/10.1126/science.3262922.

Fruman, D.A., Mather, P.E., Burakoff, S.J., Bierer, B.E., 1992. Correlation of calcineurin phosphatase activity and programmed cell death in murine T cell hybridomas. Eur. J. Immunol. 22, 2513–2517. https://doi.org/10.1002/eji.1830221008.

Groenendyk, J., Michalak, M., 2014. Disrupted WNT signaling in mouse embryonic stem cells in the absence of calreticulin. Stem Cell Rev. Rep. 10, 191–206. https://doi.org/10.1007/s12015-013-9488-6.

Guo, L., et al., 2002. Cardiac-specific expression of calcineurin reverses embryonic lethality in calreticulin-deficient mouse. J. Biol. Chem. 277, 50776–50779. https://doi.org/10.1074/jbc.M209900200.

Hu, X., et al., 2009. Src kinase up-regulates the ERK cascade through inactivation of protein phosphatase 2A following cerebral ischemia. BMC Neurosci. 10, 74. https://doi.org/10.1186/1471-2202-10-74.

Id Boufker, H., et al., 2010. The Src inhibitor dasatinib accelerates the differentiation of human bone marrow-derived mesenchymal stromal cells into osteoblasts. BMC Cancer 10, 298. https://doi.org/10.1186/1471-2407-10-298.

Karimzadeh, F., Opas, M., 2017. Calreticulin Is Required for TGF-beta-Induced Epithelial-to-Mesenchymal Transition during Cardiogenesis in Mouse Embryonic Stem Cells. Stem Cell Rep. 8, 1299–1311. https://doi.org/10.1016/j.stemcr.2017.03.018.

Khatami, M., Stramm, L.E., Rockey, J.H., 1986. Ascorbate transport in cultured cat retinal pigment epithelial cells. Exp. Eye Res. 43, 607–615. https://doi.org/10.1016/s0014-4835(86)80027-6.

Lee, K.H., et al., 2003. Calreticulin inhibits the MEK1,2-ERK1,2 pathway in alpha 1-adrenergic receptor/Gh-stimulated hypertrophy of neonatal rat cardiomyocytes. J. Steroid Biochem. Mol. Biol. 84, 101–107. https://doi.org/10.1016/s0960-0760(03)00006-2.

Lee, Y.C., et al., 2010. Src family kinase/abl inhibitor dasatinib suppresses proliferation and enhances differentiation of osteoblasts. Oncogene 29, 3196–3207. https://doi.org/10.1038/onc.2010.73.

Lynch, J., et al., 2005. Calreticulin signals upstream of calcineurin and MEF2C in a critical Ca(2+)-dependent signaling cascade. J. Cell Biol. 170, 37–47. https://doi.org/10.1083/jcb.200412156.

Lynch, J.M., Chilibeck, K., Qui, Y., Michalak, M., 2006. Assembling pieces of the cardiac puzzle; calreticulin and calcium-dependent pathways in cardiac development, health, and disease. Trend. Cardiovasc. Med. 16, 65–69. https://doi.org/10.1016/j.tcm.2006.01.004.

Lynch, J., Michalak, M., 2003. Calreticulin is an upstream regulator of calcineurin. Biochem. Biophys. Res. Commun. 311, 1173–1179. https://doi.org/10.1016/j.bbrc.2003.08.040.

Marzia, M., et al., 2000. Decreased c-Src expression enhances osteoblast differentiation and bone formation. J. Cell Biol. 151, 311–320. https://doi.org/10.1083/jcb.151.2.311.

McDonnell, P. J., Rowen, S. L., Glaser, B. M. & Sato, M. Posterior capsule opacification. An in vitro model. Arch. Ophthalmol. (Chicago, Ill.: 1960) 103, 1378-1381, doi:10.1001/archopht.1985.01050090130047 (1985).

Mesaeli, N., et al., 1999. Calreticulin is essential for cardiac development. J. Cell Biol. 144, 857–868. https://doi.org/10.1083/jcb.144.5.857.
Michalak, M., Groenendyk, J., Szabo, E., Gold, L.I., Opas, M., 2009. Calreticulin, a multi-process calcium-buffering chaperone of the endoplasmic reticulum. Biochem. J. 417, 651–666. https://doi.org/10.1042/bj20081847.
Michaylova, V., Ilkova, P., 1971. Photometric determination of micro amounts of calcium with arsenazo III. Anal. Chim. Acta 53, 194–198. https://doi.org/10.1016/S0003-2670(01)80088-X.
Murrills, R.J., et al., 2012. Osteogenic effects of a potent Src-over-Abl-selective kinase inhibitor in the mouse. J. Pharmacol. Exp. Therapeut. 340, 676–687. https://doi.org/10.1124/jpet.111.185793.
Nishida, T., et al., 1983. Fibronectin promotes epithelial migration of cultured rabbit cornea in situ. J. Cell Biol. 97, 1653–1657. https://doi.org/10.1083/jcb.97.5.1653.
Owen, T.A., et al., 1990. Progressive development of the rat osteoblast phenotype in vitro: reciprocal relationships in expression of genes associated with osteoblast proliferation and differentiation during formation of the bone extracellular matrix. J. Cellul. Physiol. 143, 420–430. https://doi.org/10.1002/jcp.1041430304.
Papp, S., Fadel, M.P., Kim, H., McCulloch, C.A., Opas, M., 2007. Calreticulin affects fibronectin-based cell-substratum adhesion via the regulation of c-Src activity. J. Biol. Chem. 282, 16585–16598. https://doi.org/10.1074/jbc.M701011200.
Papp, S., Szabo, E., Kim, H., McCulloch, C.A., Opas, M., 2008. Kinase-dependent adhesion to fibronectin: regulation by calreticulin. Exp. Cell Res. 314, 1313–1326. https://doi.org/10.1016/j.yexcr.2008.01.008.
Papp, S., Dziak, E., Opas, M., 2009. Embryonic stem cell-derived cardiomyogenesis: a novel role for calreticulin as a regulator. Stem Cells (Dayton, Ohio) 27, 1507–1515. https://doi.org/10.1002/stem.85.
Parsons, S.J., Parsons, J.T., 2004. Src family kinases, key regulators of signal transduction. Oncogene 23, 7906–7909. https://doi.org/10.1038/sj.onc.1208160.
Pilquil, C., Alvandi, Z., Opas, M., 2020. Calreticulin regulates a switch between osteoblast and chondrocyte lineages derived from murine embryonic stem cells. J. Biol. Chem. https://doi.org/10.1074/jbc.RA119.011029.
Porrello, K., LaVail, M.M., 1986. Histochemical demonstration of spatial heterogeneity in the interphotoreceptor matrix of the rat retina. Investig. Ophthalmol. Vis. Sci. 27, 1577–1586.
Soriano, P., Montgomery, C., Geske, R., Bradley, A., 1991. Targeted disruption of the c-src proto-oncogene leads to osteopetrosis in mice. Cell 64, 693–702. https://doi.org/10.1016/0092-8674(91)90499-o.
Sun, L., et al., 2005. Calcineurin regulates bone formation by the osteoblast. PNAS 102, 17130–17135. https://doi.org/10.1073/pnas.0508480102.
Szabo, E., Papp, S., Opas, M., 2007. Differential calreticulin expression affects focal contacts via the calmodulin/CaMK II pathway. J. Cellul. Physiol. 213, 269–277. https://doi.org/10.1002/jcp.21122.
Szabo, E., Soboloff, J., Dziak, E., Opas, M., 2009. Tamoxifen-inducible Cre-mediated calreticulin excision to study mouse embryonic stem cell differentiation. Stem Cells Dev. 18, 187–193. https://doi.org/10.1089/scd.2008.0064.
Szabo, E., Feng, T., Dziak, E., Opas, M., 2009. Cell adhesion and spreading affect adipogenesis from embryonic stem cells: the role of calreticulin. Stem Cells (Dayton, Ohio) 27, 2092–2102. https://doi.org/10.1002/stem.137.
Tomita, M., Reinhold, M.I., Molkentin, J.D., Naski, M.C., 2002. Calcineurin and NFAT4 induce chondrogenesis. J. Biol. Chem. 277, 42214–42218. https://doi.org/10.1074/jbc.C200504200.
Toyoshima, S., Saito, T., Yamaguchi, J., 1986. Immuno-scanning electron microscopy of macrophage cytoskeleton by using colloidal gold and backscattered electron imaging mode. J. Electron Microsc. 35, 247–258.
Wee, H.J., Huang, G., Shigesada, K., Ito, Y., 2002. Serine phosphorylation of RUNX2 with novel potential functions as negative regulatory mechanisms. EMBO Rep. 3, 967–974. https://doi.org/10.1093/embo-reports/kvf193.
Winslow, M.M., et al., 2006. Calcineurin/NFAT signaling in osteoblasts regulates bone mass. Dev. Cell 10, 771–782. https://doi.org/10.1016/j.devcel.2006.04.006.
Yu, Y., Pilquil, C., Opas, M., 2016. Osteogenic Differentiation from Embryonic Stem Cells. Method. Mol. Biol. (Clifton N.J.) 425–435. https://doi.org/10.1007/7651_2014_126.